

Interpreting the Colour-Magnitude Diagrams of Open Star Clusters through Numerical Simulations

Jasonjot Singh Kalirai^{1*} and Monica Tosi^{2*}

¹*Department of Physics & Astronomy, 6224 Agricultural Road, University of British Columbia, Vancouver BC V6T1Z1*

²*INAF - Osservatorio Astronomico di Bologna, Via Ranzani 1, I-40127 Bologna, Italy*

Accepted 2004 March 08. Received 2004 January 13; in original form 2004 January 13

ABSTRACT

We present detailed comparisons between high quality observational colour-magnitude diagrams (CMDs) of open star clusters and synthetic CMDs based on MonteCarlo numerical simulations. The comparisons account for all of the main parameters which determine the shape of the CMD for a stellar population. For the four clusters studied, NGC 6819, NGC 2099 (M37), NGC 2168 (M35) and NGC 2323 (M50), we derive reddening, distance, age, binary fraction, star formation rate and indicative metallicity by comparing the locations and density of points in the observed CMDs to the simulated CMDs. We estimate the uncertainties related to stellar evolution theories by adopting various sets of stellar models for all of the synthetic CMDs and discuss which stellar models provide the theoretical CMDs that best reproduce the observations.

Key words: colour-magnitude diagrams – methods: n-body simulations – open clusters and associations: general – open cluster and associations: individual: NGC 2099, NGC 2168, NGC 2323, NGC 6819

1 INTRODUCTION

Theoretical isochrones are commonly fit to the major observational sequences of star clusters in order to both better understand the underlying physics of stellar evolution and to determine properties of the clusters, i.e., the age. If the metallicity, reddening and distance to the cluster are well constrained from independent techniques, the comparisons typically involve matching the morphology of the turn-off and location of the red giant stars to predictions. Recently, the newer method of using synthetic colour-magnitude diagrams to compare with observational data has proven to be much more informative and rewarding (Aparicio et al. 1990; Tosi et al. 1991; Skillman & Gallart 2002). These Monte-Carlo simulations allow modelling of several additional parameters which dictate the distribution of points in the CMD, such as stochastic star formation (SF) processes, binary fraction, photometric spread, main-sequence thickness, data incompleteness and small number statistics. Consequently, the results not only provide a measure of the properties of the cluster, but can also constrain the star formation history (SFH) and the initial mass function (IMF). Furthermore, by comparing the simulations based on several different sets of evolutionary tracks, we can constrain which models use the best prescription of parameters (such as treatment of overshooting, mixing length, etc...).

Confronting the simulations with observations requires a large data set with accurate photometry. For this, we use the deep BV photometry presented in the CFHT Open Star Cluster Survey (Kalirai et al. (2001a), hereafter JSKI). JSKI observed 19 open star clusters in our Galaxy and have yet published results on the four richest clusters, NGC 6819 (Kalirai et al. (2001b), hereafter JSKII), NGC 2099 (Kalirai et al. (2001c), hereafter JSKIII), and NGC 2168 and NGC 2323 (Kalirai et al. (2003), hereafter JSKIV). These data were reduced and calibrated in a homogenous manner as described in JSKI. The resulting CMDs exhibit very tight main sequences showing several ‘kinks’ and slope changes which are predicted by theory. More importantly, the combination of very short and deep exposures, and the large aerial coverage of the detector ($42' \times 28'$) has allowed the measurement of stars from the brightest asymptotic giant branch (AGB) and red giant branch (RGB) phases down to very low-mass main-sequence phases ($\sim 0.2 M_{\odot}$). This allows our comparisons to yield evolutionary information over a wide mass range.

The reduced data set in the CFHT Open Star Cluster Survey has been requested by, and made available to, several investigators for additional science rewards outside our goals (e.g., astrometric studies, proper motions, variable stars, radial velocities, brown dwarfs, blue stragglers and Galactic disk star distributions). The present study complements these efforts and analyses the four published clusters in a way that allows us to include them in a large homo-

* E-mail: jkalirai@physics.ubc.ca; tosi@bo.astro.it

geneous sample of open clusters aimed at studying the formation and evolution of the Galactic disk (Bragaglia 2003, and references therein). Galactic open clusters are indeed particularly well suited to this purpose, since they span a range of ages from a few million to several billion years and can be observed in various regions of the Galactic disk characterised by different star formation histories. They can be used to study both the present day disk structure and its temporal evolution (Janes & Phelps 1994, Friel 1995, Tosi 2000, Bellazzini et al. 2003). Old open clusters offer a unique opportunity to trace the whole kinematical and chemical history of our disk, if collected in populous and representative samples and accurately and homogeneously analysed (see e.g., Twarog, Ashman, & Anthony-Twarog 1997; Carraro, Ng, & Portinari 1998).

Here we apply the synthetic CMD method to NGC 6819, NGC 2099, NGC 2168 and NGC 2323 to derive their age, reddening, distance modulus and (approximate) metallicity homogeneously to the Bragaglia (2003) cluster sample. The method also allows us to determine other features of these clusters, such as the existence (or lack thereof) of a significant fraction of unresolved binary systems, the original total mass of formed stars and the possible evaporation of some of the lower mass stars.

The organisation of the paper is as follows, §2 briefly summarises the data and the reduction procedures. Further details are given in JSKI. In §3 we present a summary of our main results which relate to this work from the published papers in the CFHT Open Star Cluster Survey. §4 sets up the numerical simulations and presents details on how the synthetic CMDs were created. Next, we compare the CMDs and the corresponding luminosity functions from the observations with the simulations on a cluster-by-cluster basis (§5). Finally, we discuss the results in §6 and conclude the study in §7.

2 THE OBSERVATIONAL DATA

An absolute requirement in using different data sets to make detailed comparisons between observations and models is that of homogeneity. To truly understand the variations in the different models parameters, we must minimize systematic errors. Therefore, we desire a rich data set of open clusters, all reduced using the same approach, calibrated consistently, and with well determined incompleteness factors. The richest clusters from the CFHT Open Star Cluster Survey, NGC 6819, NGC 2099 (M37), NGC 2168 (M35) and NGC 2323 (M50) perfectly meet these requirements. The data were all imaged during an excellent three night observing run with the Canada-France-Hawaii Telescope (CFHT) on 1999 October, using the CFH12K camera. The optical detector is a high resolution (1×10^8 pixels) CCD mosaic camera which projects to an aerial coverage of $42' \times 28'$ on the sky.

Most clusters were observed with exposure times sufficient to reach the magnitude of the coolest white dwarfs and of the faintest M-type stars on the main sequence. We also complemented the deep photometry with shorter exposures to cover the brighter turn-off and evolved stars. The individual images were registered and co-added (where necessary) using the FITS Large Images Processing Software (FLIPS)

(J.-C. Cuillandre, 2000, Private Communication). Details of this procedure, as well as the pre-processing of the data are provided in §3 of JSKI.

The actual photometry of the sources in the images was measured using Point-Spread-Function Extractor (PSFex), a highly automated program which will be integrated in the code of a future SExtractor version (Bertin & Arnouts 1995; E. Bertin 2000, private communication). We used a separate PSF on each CCD of the mosaic. Included in the PSF are polynomial basis functions which can map the variations of the PSF across the CCD. PSFex is discussed further in §4 of JSKI.

Data for each of the clusters were taken in the *B* and *V* filters, and calibrated in the Johnson photometric system using multiple images of the SA-92 and SA-95 standard star fields (Landolt 1992). The final averaged uncertainties in the zero-point terms were measured to be ~ 0.018 magnitudes, uncertainties in the airmass coefficients were ~ 0.015 magnitudes in *V* and ~ 0.007 magnitudes in *B*. Colour coefficients, as well as airmass terms, were similar to nominal CFHT expectations. Details of the calibration of instrumental magnitudes to real magnitudes are provided in §5 and Tables 2 and 3 of JSKI.

The resulting, calibrated CMDs for the open clusters exhibit unprecedented long, clear main sequences ranging from the brightest cluster members to the limiting magnitude in each case ($23 \leq V \leq 25$). A summary of the observational log for each cluster (exposure time, seeing, airmass, etc...) is presented in Table 1.

3 FIRST RESULTS: ISOCHRONE FITTING

Figure 1 presents the final calibrated CMDs for each of the four open clusters, with the best fit theoretical isochrones as determined in our previous published analysis of these clusters (see JSKII, JSKIII, JSKIV for details). These rich clusters are clearly delineated from the background Galactic disk stars. The main sequences are very tight and show several features which are predicted by stellar evolutionary theory (see §5). For this, we used a new grid of model isochrones calculated by the group at the Rome Observatory according to the prescription described in Ventura et al. (1998). These models adopt convective core-overshooting by means of an exponential decay of the turbulent velocity out of the formal convective borders fixed by Schwarzschild's criterion; a free parameter which gives the e-folding distance of the exponential decay is set to $\zeta = 0.03$ (Ventura et al. 1998). The convective flux has been evaluated according to the Full Spectrum of Turbulence (FST) theory prescriptions (Canuto & Mazzitelli 1992). The theoretical isochrones were transformed into the observational plane by making use of the Bessel, Castelli & Pletz (1998) conversions. The lower main sequence ($M \lesssim 0.7 M_{\odot}$) was calculated by adopting NextGen atmosphere models (Hauschildt, Allard & Baron 1999). For $M \lesssim 0.47 M_{\odot}$ (or $T_{\text{eff}} \lesssim 3500$ K) the transformations of Hauschildt, Allard & Baron (1999) in *B-V* are not very reliable and so the faint end of the isochrones terminate at this mass. These models will be referred to as FST from here on.

Table 1. Observational Data for NGC 6819, NGC 2099 (M37), NGC 2168 (M35) and NGC 2323 (M50)

| Cluster | Filter | Exposure Time (s) | No. of Images | Seeing (") | Airmass |
|----------------|--------|-------------------|---------------|------------|-----------|
| NGC 6819 | | | | | |
| | V | 300 | 9 | 0.7 | 1.3 |
| | V | 50 | 1 | 0.7 | 1.16 |
| | V | 10 | 1 | 0.68 | 1.15 |
| | V | 1 | 1* | 0.78 | 1.27 |
| | B | 300 | 9 | 0.9 | 1.40-1.76 |
| | B | 50 | 1 | 0.82 | 1.38 |
| | B | 10 | 1 | 0.84 | 1.37 |
| | B | 1 | 1* | 1.1 | 1.25 |
| NGC 2099 | | | | | |
| | V | 300 | 3 | 0.85 | 1.03 |
| | V | 50 | 1 | 0.97 | 1.04 |
| | V | 10 | 1 | 0.99 | 1.04 |
| | V | 0.5 | 1* | 1.1 | 1.19 |
| | B | 300 | 3 | 0.79 | 1.03 |
| | B | 50 | 1 | 0.85 | 1.03 |
| | B | 10 | 1 | 0.85 | 1.03 |
| | B | 0.5 | 1* | 1.0 | 1.19 |
| NGC 2168 | | | | | |
| | V | 300 | 1 | 1.35 | 1.6 |
| | V | 50 | 1 | 1.35 | 1.6 |
| | V | 10 | 1 | 1.35 | 1.6 |
| | V | 1 | 1* | 1.2 | 1.35 |
| | V | 0.5 | 1* | 1.2 | 1.35 |
| | B | 300 | 1 | 1.2 | 1.6 |
| | B | 50 | 1 | 1.2 | 1.6 |
| | B | 10 | 1 | 1.2 | 1.6 |
| | B | 1 | 1* | 1.1 | 1.35 |
| | B | 0.5 | 1* | 1.1 | 1.35 |
| NGC 2323 | | | | | |
| | V | 300 | 1 | 0.85 | 1.15 |
| | V | 50 | 1 | 0.85 | 1.15 |
| | V | 10 | 1 | 0.85 | 1.15 |
| | V | 1 | 1* | 1.0 | 1.2 |
| | V | 0.5 | 1* | 1.0 | 1.2 |
| | B | 300 | 1 | 0.95 | 1.15 |
| | B | 50 | 1 | 0.95 | 1.15 |
| | B | 10 | 1 | 0.95 | 1.15 |
| | B | 1 | 1* | 1.1 | 1.2 |
| | B | 0.5 | 1* | 1.1 | 1.2 |

1. * These very short exposures were obtained at a later date.

3.1 Published Results – NGC 6819

The tight, very rich, main sequence and turn-off consist of over 2900 cluster stars to our limiting magnitude. Main-sequence fitting of the un-evolved cluster stars with the Hyades star cluster yields a distance modulus of $(m-M)_V = 12.30 \pm 0.12$ ($d = 2500$ pc), for a reddening of $E(B-V) = 0.10$. These values are consistent with a theoretical isochrone of age 2.5 Gyrs. Detailed star counts in concentric annuli out to large angular radii set constraints on the cluster radius, $R = 9'.5 \pm 1'.0$, and clearly indicates mass segregation in the cluster. The global cluster mass function is found to be quite flat, $x = -0.15$ ($x = 1.35$, Salpeter). A large population of white dwarf stars is found in the cluster and is currently being investigated spectroscopically.

3.2 Published Results – NGC 2099 (M37)

The cluster CMD shows extremely well populated and very tightly constrained main sequence, turn-off, and red giant populations. The photometry for this cluster is faint enough ($V \sim 24.5$) to detect the end of the white dwarf cooling sequence. Therefore, the white dwarfs are used as chronometers to age the cluster providing an independent age ($566 \pm \frac{154}{176}$ Myrs) from the main-sequence turn-off plus red giant clump fit (520 Myrs). We also derive the reddening ($E(B-V) = 0.21 \pm 0.03$) and distance ($(m-M)_V = 11.55 \pm 0.13$) to NGC 2099 by matching main-sequence features in the cluster to a fiducial main-sequence for the Hyades (de Bruijne, Hoogerwerf & de Zeeuw 2001), after correcting for small metallicity differences. The cluster luminosity and mass functions indicate some evidence for mass segregation within the boundary of the cluster.

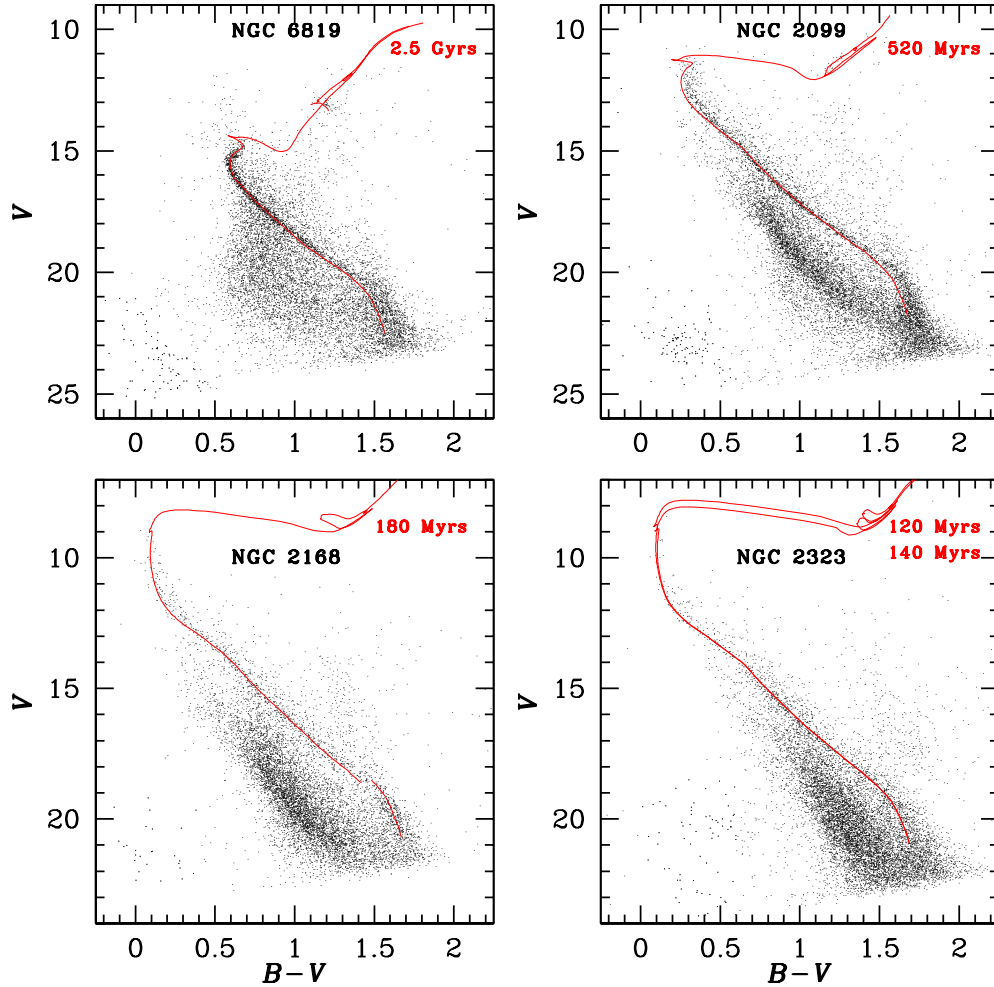


Figure 1. Isochrone fits for each cluster are shown with corresponding ages. All models are Solar metallicity with the exception of NGC 2168, for which $Z = 0.012$. For the lower main sequence, we were not able to compute non-grey atmospheres for this metallicity. We therefore overplot the lower main sequence from a Solar metallicity model (bottom-left).

3.3 Published Results – NGC 2168 (M35)

NGC 2168 is a well studied nearby ($d = 912 \pm \frac{70}{65}$ pc) young cluster (180 Myrs) showing a well defined main sequence. The reddening of the cluster, $E(B-V) = 0.20$, and the metallicity, $Z = 0.012$, were adopted from the literature (Sarrazine et al. 2000; Barrado y Navascués, Deliyannis & Stauffer 2001). The cluster is found to contain ~ 1000 stars above our limiting magnitude with a global mass function slope very similar to a Salpeter value ($x = 1.29$). There is mild evidence for mass segregation in the cluster. White dwarf stars are found and can potentially set very important constraints on the high-mass end of the white dwarf initial-final mass relationship considering they must have evolved from quite massive progenitors.

3.4 Published Results – NGC 2323 (M50)

NGC 2323 is one of the youngest clusters in the CFHT Open Cluster Survey (130 Myrs), and shows a main sequence extending over 14 magnitudes in the $V, B-V$ plane. The cluster

has had very few photographic/photoelectric studies, and prior to our efforts, no previously known CCD analysis. This is surprising considering the rich stellar population (~ 2100 stars above our magnitude limit) and the relatively low distance modulus ($(m-M)_0 = 10.00 \pm 0.17$). The cluster shows clear evidence of mass segregation, an important result considering the dynamical age is only $1.3\times$ the cluster age.

4 SYNTHETIC COLOUR-MAGNITUDE DIAGRAMS

Age, reddening and distances for the four clusters have been re-derived applying the synthetic CMD method (Tosi et al. 1991) to the empirical CMDs described above. The best values of the parameters are found by selecting the values that provide synthetic CMDs with morphology, number of stars in the various evolutionary phases and luminosity functions in better agreement with the empirical ones. The method has already been successfully applied to several clusters (Bragaglia 2003 and references therein).

The synthetic CMDs are constructed via MonteCarlo

extractions of (mass, age) pairs, according to an assumed IMF, SF law, and time interval of the SF activity. Each extracted synthetic star is placed in the CMD by suitable interpolations on the adopted stellar evolution tracks and adopting the Bessel et al. (1998) tables for photometric conversion in the Johnson-Cousins photometric system. The absolute magnitude is converted to a *provisional* apparent magnitude by applying (arbitrary) reddening and distance modulus. The synthetic stars extracted for any magnitude and photometric band are assigned the photometric error derived for the actual stars of the same apparent magnitude. Then, they are randomly retained or rejected on the basis of the incompleteness factors of the actual data, derived from extensive artificial star tests.

Once the number of objects populating the whole synthetic CMD (or portions of it) equals that of the observed one, the procedure is stopped, yielding the quantitative level of the SF rate consistent with the observational data, for the prescribed IMF and SF law. To evaluate the goodness of the model predictions, we compare them with: the observational luminosity functions, the overall morphology of the CMD, the stellar magnitude and colour distributions, the number of objects in particular phases (e.g., on the red giant branch, in the clump, on the blue loops, etc.). A model can be considered satisfactory only if it reproduces all of the features of the empirical CMDs and luminosity functions. Given the uncertainties affecting both the photometry and the theoretical parameters (stellar evolution tracks included), the method cannot provide strictly unique results; however, it allows us to significantly reduce the range of acceptable parameters.

In this way we derive the age, reddening, distance of the cluster, and indicate the metallicity of the stellar evolution models in better agreement with the data. In principle, the latter should be indicative of the cluster metallicity, but this depends significantly on some of the stellar model assumptions, such as opacities.

To estimate if, and how many, unresolved binary systems could be present in the cluster, the synthetic CMDs have been computed both assuming that all the cluster stars are single objects and that an (arbitrary) fraction of them are members of binary systems with random mass ratio. Again, the comparison of the resulting main-sequence morphology and thickness with the observed ones allows us to derive information on the most likely fraction of binaries.

We also infer the astration mass of the cluster (i.e., the total mass that went in all of the stars formed in the cluster), according to the adopted IMF. The method here also allows us to derive the best IMF as long as the observed mass range of main-sequence stars is sufficiently large and the main sequence is sufficiently tight. However, the high background contamination affecting the systems examined here and the lack of sufficiently reliable external blank fields, make the derivation too unsafe to discuss it here. Other factors (see below), such as the actual size of the photometric errors also prevents us from comparing the IMF in any significant detail.

5 OBSERVATIONS VS THEORY - COLOUR-MAGNITUDE DIAGRAMS AND LUMINOSITY FUNCTIONS

To test the effect of different input physics on the derived age, reddening and distance modulus, we have run the simulations with three different sets of stellar evolutionary tracks. The adopted sets were chosen because they assume different prescriptions for the treatment of convection and range from no overshooting to rather high overshooting from convective regions. Despite these differences, they are all able to well reproduce the observed CMDs of both star clusters and nearby galaxies. They are thus suitable to evaluate the intrinsic uncertainties still related to stellar evolution models. We use the FST tracks of Ventura et al. (1998) with high ($\zeta = 0.03$) and moderate ($\zeta = 0.02$) overshooting; the BBC94 tracks of the Padova group (Bressan et al. 1993; Fagotto et al. 1994), with overshooting; and the FRANEC tracks (Dominguez et al. 1999) with no overshooting. For those cases where the metallicities are not well constrained, we allow different values in our comparisons. Incompleteness factors and photometric errors are taken from the original papers in the CFHT Open Star Cluster Survey series (JSKII, JSKIII and JSKIV) and folded into the numerical simulations.

All models assume that the star formation activity has lasted 5 Myr (i.e., approximately an instantaneous burst) and that the stars were formed following a single slope ($x = 1.35$) Salpeter's IMF over the whole mass range covered by the adopted tracks (0.6 – 100 M_{\odot}).

Figures 2, 4, 6 and 8 show for each cluster the synthetic models in better agreement with the data for each adopted set of stellar tracks, as well as the cluster observational CMD on the same scale. In all of these figures the CMDs in the top row are the synthetic ones, those in the second row are the same synthetic ones but overlapped with the stars of the equal area fiducial blank field, and the bottom CMD is the empirical one. Figures 3, 5, 7 and 9 compare the empirical luminosity functions with those predicted by the best synthetic models. Ultimately, the best models have been selected by visually comparing features between the synthetic models and the observations, such as the location and density of points on the CMD. However, we have also attempted to confirm our results by using both the two-dimensional Kolmogorov-Smirnov test on the CMD and χ^2 tests on the luminosity and colour functions. In the cases of well constrained field contamination, such as behind NGC 6819 and NGC 2099, the tests confirm our choices of best synthetic models. For the other two clusters, the tests do not help discriminate between best choice of models and we strictly use conclusions based on the visual location of points. Also, these statistical tests are particularly not well suited for these comparisons because of the insignificant weight given to the small number of stars in key evolutionary stages which must be fit by the synthetic models (such as the red giant clump).

5.1 NGC 6819

NGC 6819 is the richest cluster in this work. The cluster field contains 10510 *bona fide* stars (i.e., with *stellarity* parameter ≥ 0.5) while the blank field of same area contains 8504 *bona*

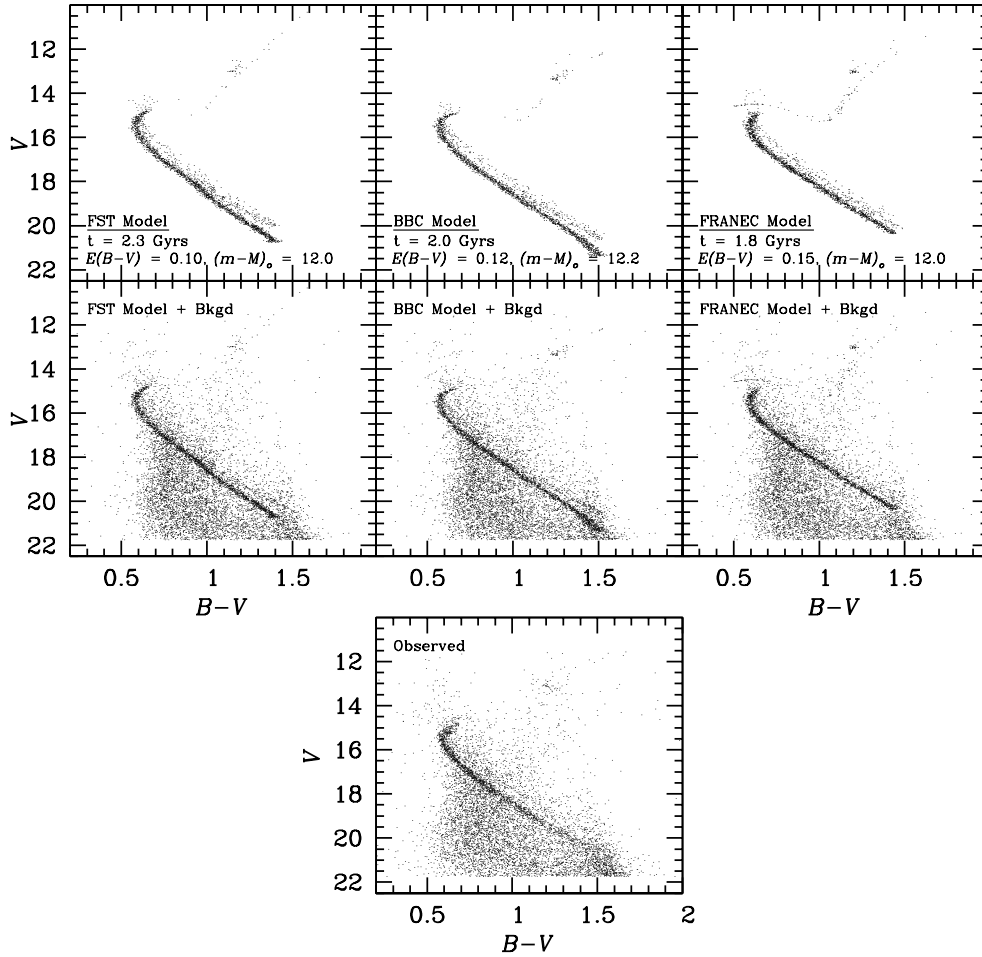


Figure 2. Synthetic CMDs with $Z = 0.02$ and a 20% binary fraction (random mass ratio) are shown for NGC 6819. The BBC94 tracks are found to provide the best agreement with the observations (bottom panel). The data has been truncated at the faintest magnitudes (see Figure 1 for full CMD). See §5.1 for more information.

fide stars. The synthetic CMDs are therefore computed with 2000 objects (a fraction of which are assumed to be members of binary systems).

All of the tracks used to simulate the NGC 6819 CMD are Solar metallicity models as the cluster metallicity has been constrained to this value through the high resolution analysis of Bragaglia et al. (2001). Figure 2 shows that the three sets of models provide slightly different ages (and hence, reddening and distances), which strictly depend on the assumed amount of overshooting: the higher the overshooting, the older the age. This is of course due to higher overshooting models having higher stellar luminosities, thus allowing lower mass stars to reach the desired luminosity. The variations in the ages seen in the models also stress the importance of deriving uncertainties on cluster parameters by using different sets of tracks.

The FST models with $\zeta = 0.03$ (left) lead to parameters virtually identical to those found in JSKII. A better estimate of the age is found to be 2.30 ± 0.15 Gyrs, distance modulus $(m-M)_o = 12.0$, and reddening $E(B-V) = 0.10$. The FRANEC models (right) suggest younger ages, due to their lack of overshooting, 1.6-1.8 Gyrs, and therefore need

a slightly higher reddening ($E(B-V) = 0.15$) to reproduce the colours. The BBC94 models (middle), with intermediate overshooting, favor an intermediate age of 2.0 Gyrs, with $E(B-V) = 0.12$ and $(m-M)_o = 12.2$.

None of these models are found to perfectly reproduce all of the observed features in the NGC 6819 CMD. For example, the FST models predict a main-sequence slope steeper than the observed one and the two diverge at the faint end. These models also tend to place the red giant clump excessively towards the red, probably due to the fact that the models don't include mass loss. The FRANEC models better reproduce the main-sequence distribution but present a turn-off with a hook that is too pronounced, a likely consequence of the young age. Given the high field contamination, however, this feature is not particularly evident in the combined CMDs of the second row. A smaller cluster core CMD shows the hook prominently. The FRANEC models also overpopulate the lower red giant branch. This is visible even despite the fact that this region of the CMD is plenty of contaminating objects. The BBC94 models provide the best fit to the data CMD, despite a main-sequence slope which is slightly too steep. Most of these discrepancies

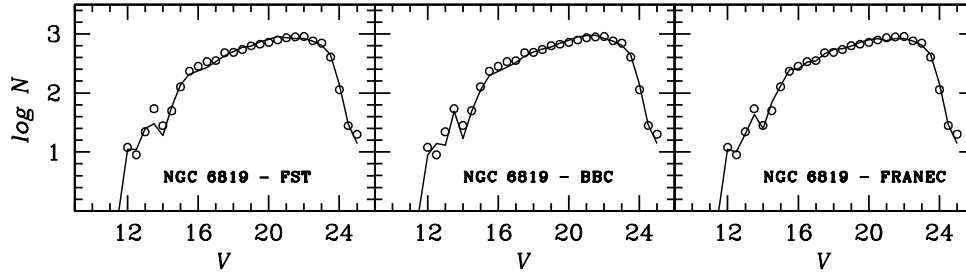


Figure 3. The empirical NGC 6819 luminosity function (open circles) is compared with the predicted luminosity function from the numerical simulations (solid line). See §5.1 for a discussion of these results.

between the observed features and the synthetic CMDs result from problems in the stellar models. As pointed out by Andreuzzi et al. (2004) studying the open cluster NGC 6939 with the same method, assuming a reddening dependence on the stellar colour as adopted by Twarog et al. (1997) makes the synthetic main sequences even steeper and, hence, more inconsistent with the data.

Another evident result that we find for all of the clusters studied here, is that the observed main-sequence spread cannot be reproduced if one assumes photometric errors as small as those listed in our photometry catalogue. To test the actual size of the photometric errors we revert back to the artificial star tests presented in JSKII. A plot of the $V_{in} - V_{out}$ distribution tells us that, in fact, the errors quoted agree with the artificial star tests. The synthetic CMDs however, require that either the errors are larger, at least 0.01 magnitude even in the brighter bins, or there is some physical cause for the observed spread (i.e., differential reddening or metallicity spread). A spread due to binaries is modelled and therefore ruled out as a cause for this discrepancy. The apparent spread could be caused by small offsets in the calibration of the different CCDs of the mosaic, but internal metallicity spread in the cluster or small differential reddening cannot be excluded. We are currently investigating this possibility in another project (R. S. French et al. 2003, private communication). For now, we have increased the errors to 0.01 magnitude for stars brighter than $V = 19$ and doubled them for fainter bins ($\sigma = 0.01$ at $V = 21$, $\sigma = 0.04$ at $V = 23$). Empirically, this is the minimum size required to obtain a main-sequence spread comparable with the observed one.

All of the shown cases in Figure 2 assume that 20% of the stars are in binary systems with random mass ratio. We also tested simulations with 30% binaries and found minor differences. Given the high field contamination, it is difficult to understand which fraction and assumption of the mass ratio is the best case. It could entirely be true that the fraction is actually smaller if the mass ratio is more skewed towards equal masses. Models without binaries are not shown as they amplify the problem of the main-sequence width (the predicted one is too tight) and do not correctly reproduce the stellar distribution on the red side of the main sequence.

Figure 3 shows the empirical luminosity function of the 10510 cluster field stars (empty circles) compared to the luminosity functions resulting from the sum of the 2000 synthetic stars of Figure 2 with the 8504 stars of the blank field.

The agreement is excellent, except for the slight underestimate of the clump stars of the FST models.

A clear result of our study is that all of the synthetic CMDs for NGC 6819 show overpopulated faint main sequences ($V > 20$), both for single and binary stars. This is a clear signature of low mass stellar evaporation (or at least segregation outwards of our cluster boundary, 9'5). As we showed in JSKII, the mass function of this cluster steadily marches to flatter values, and becomes inverted in the outermost annuli. Therefore, the observations provide the answer to this overabundance. However the effect is not seen in the luminosity function comparisons, which are in excellent agreement with the observed one. This suggests either that the faint magnitude luminosity function is dominated by field contamination or that the apparent over-concentration of the synthetic main sequences is actually an artifact of the residual underestimate of the photometric errors.

Assuming a single slope Salpeter IMF, the mass of gas that formed the stars of the surveyed area of NGC 6819 between 0.6 and $100 M_{\odot}$ is $\simeq 4.2 \times 10^3 M_{\odot}$ with the BBC94 models, $4.0 \times 10^3 M_{\odot}$ and $4.9 \times 10^3 M_{\odot}$ with the FST and the FRANEC models, respectively. Hence, different stellar models do not provide the same answer for a global parameter such as the star formation either. The differences are again related to the adopted input physics and to the amount of assumed overshooting in the stellar models. Less overshooting implies higher masses for the observed living stars, i.e. shorter lifetimes, which, convolved with the negative slope of the IMF, leads to a higher total astrated mass.

5.2 NGC 2099

The cluster field contains 12194 *bona fide* stars, while the blank field extrapolated to the cluster area contains 10576 stars. Hence, the synthetic CMDs have been computed with 1618 objects.

In JSKIII, we assumed the cluster metallicity of NGC 2099 to be Solar, based on the isochrone fitting results of Mermilliod et al. (1996) as well as our own best guess from the fit. A more recent study, Nilakshi & Sagar (2001), prefer a subsolar $Z = 0.008$ metallicity, again based on isochrone fitting. Therefore, one goal is to constrain the metallicity of the cluster based on synthetic CMD comparisons. So, for this cluster we use the the FST tracks of Ventura et al. (1998) with $\zeta = 0.03$, $Z = 0.02$ and $Z = 0.006$, the BBC94 tracks of the Padova group with $Z = 0.02$ (Bressan et al. 1993) and $Z = 0.008$ (Fagotto et al. 1994), and the FRANEC tracks

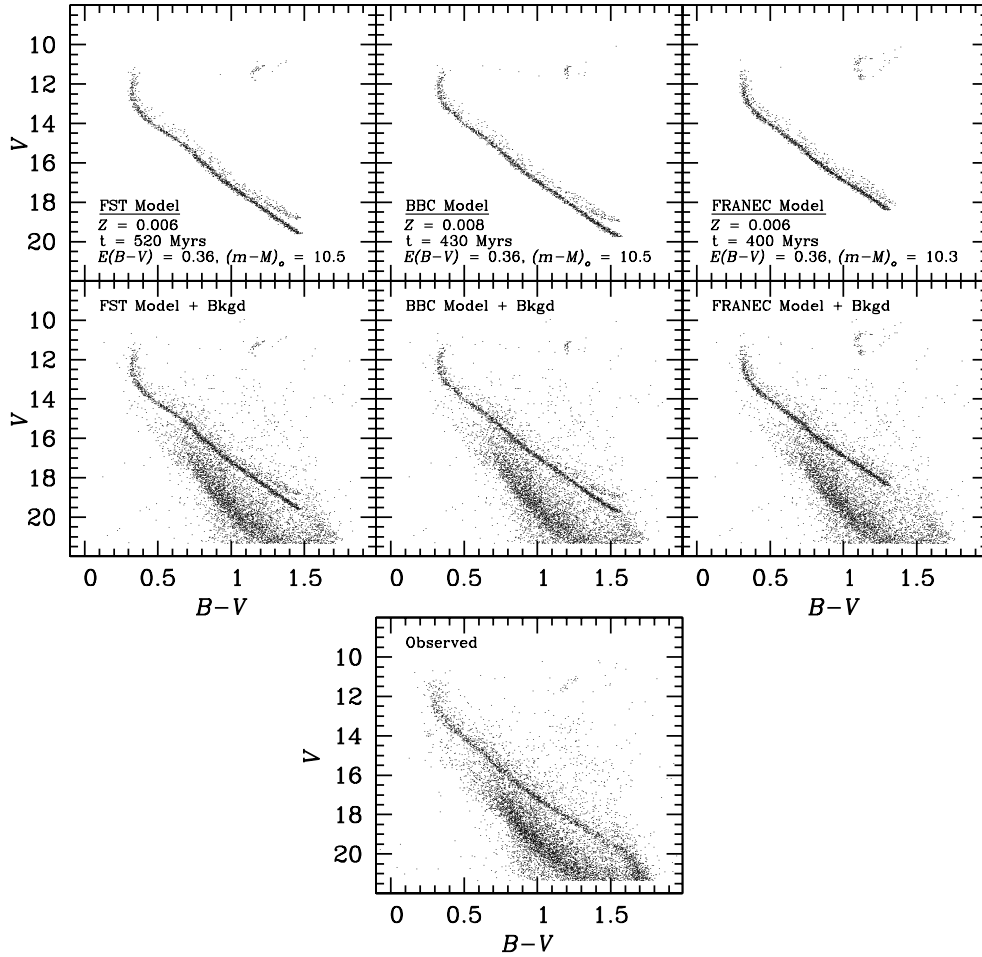


Figure 4. Synthetic CMDs with subsolar metallicities and a 20% binary fraction (random mass ratio), are shown for NGC 2099. The BBC94 tracks are found to provide the best agreement with the observations (bottom panel). The data has been truncated at the faintest magnitudes (see Figure 1 for full CMD). See §5.2 for more information.

(Dominguez et al. 1999) with $Z = 0.02$, $Z = 0.01$ and $Z = 0.006$.

For the FST, the synthetic sequences using Solar metallicity models look impressively consistent with the observed CMD in all the minimal details. However, the turn-off and clump shape are not very good: the sequence after the turn-off is too long and curved and the clump is a bit short and faint. It is also very difficult to single out the best age, as anything between 520 and 700 Myrs doesn't significantly change the important CMD features (clump morphology and luminosity, shape of turn-off, etc...), all looking reasonable. The clump becomes too faint below 500 Myrs, indicating that this is a lower age limit and too blue beyond 800 Myrs indicating an upper limit. The best fit resulting parameters for these tracks are therefore age = 620 ± 60 Myrs, $E(B-V) = 0.21 \pm 0.02$, and $(m-M)_o = 10.70 \pm 0.20$. The BBC94 $Z = 0.02$ tracks excellently reproduce all of the main sequence and clump features, but have long post turn-off sequences, as we saw in the FST models. For Solar metallicity, these tracks are in better agreement with the data than the FST models. The age is also better constrained, thanks to a higher sensitivity of the various features: age = 590 ± 10

Myrs, $E(B-V) = 0.18 \pm 0.01$, and $(m-M)_o = 10.50 \pm 0.10$. The FRANEC $Z = 0.02$ tracks provide the best agreement with the observed upper main sequence and turn-off features. However, the resulting clump is too vertical and overpopulated. Part of the latter problem is due to the fact that their main sequence is not as deep as the others, because the minimum mass available to us is $0.7 M_\odot$, instead of $0.6 M_\odot$ as for the FST and Padova models. The code therefore can not distribute the required 1618 faint stars in these bins and, inevitably, puts a larger number of brighter stars according to a Salpeter IMF. The resulting best fit parameters in the FRANEC models are age = 590 ± 10 Myrs, $E(B-V) = 0.16 \pm 0.02$, and $(m-M)_o = 10.31 \pm 0.10$.

Figure 4 presents the lower metallicity synthetic CMDs for NGC 2099. For the $Z = 0.006$ FST models (left), the length of the sequence just after the turn-off shortens and becomes more vertical, thus better reproducing the observed morphology. The clump morphology also improves, thanks to a slightly larger extension. However, the agreement in the main-sequence morphology is no longer as excellent as the higher metallicity case, but still quite good. It may well be that intermediate metallicity tracks would work even better.

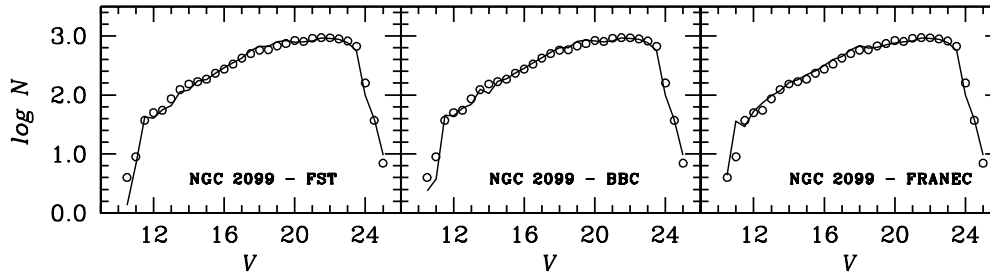


Figure 5. The empirical NGC 2099 luminosity function (open circles) is compared with the predicted luminosity function from the numerical simulations (solid line). See §5.2 for a discussion of these results.

Therefore, overall the synthetic CMDs from the FST tracks prefer the lower metallicity, with parameters: age = 520 ± 40 Myrs, $E(B-V) = 0.36 \pm 0.01$, $(m-M)_\odot = 10.40 \pm 0.10$. The BBC94 lower metallicity tracks (middle), $Z = 0.008$, are the best models for this cluster. They reproduce all of the main-sequence features and also have a better shaped turn-off than with the Solar metallicity models. A minor inconsistency is seen in the location of the clump, which is slightly too vertical, but this is a minor detail. The age is less well defined, with final best parameters age = 430 ± 30 Myrs, $E(B-V) = 0.36 \pm 0.03$, $(m-M)_\odot = 10.50$. The lower metallicity FRANEC tracks (right) can be ruled out as both the $Z = 0.01$ and $Z = 0.006$ models show extremely extended clumps (real blue loops) which are inconsistent with the observed clump for any reasonable age. Also, the lifetimes in that phase favor the stars to reside on the blue side of the clump (vertical), adding further inconsistency to the colour and shape.

We have also performed several tests on the fraction of binary stars in NGC 2099. At first glance, the empirical CMD doesn't show any evidence of binaries, but we have found a posteriori that, without including them in the synthetic CMDs, both the turn-off morphology and the colour distribution on the red side of the main sequence are not well reproduced. Our best guess is that binaries are around 15-20% of the cluster stars and all of the results that we have discussed above assume this fraction (20%) with a random mass ratio.

Figure 5 shows the empirical luminosity function of the 12194 cluster field stars (empty circles) compared to the luminosity functions resulting from the sum of the 1618 synthetic stars of Figure 4 (subsolar metallicity) with the 10576 stars of the extrapolated blank field. The predicted luminosity functions are consistent with the data, but the agreement at the brightest magnitudes is not exceptional. The very good match at the faintest magnitudes shows that the extrapolation of the number of stars observed in the blank field to the larger area covered by the cluster is correct.

The general fits of the data to synthetic CMDs favor the lower metallicity models for NGC 2099, thus requiring a higher reddening. These are found to better reproduce the shape of the upper main sequence and turn-off. Notice that age and modulus derived here do not coincide with those derived JSKIII with the same stellar tracks. The difference in age is probably due to the fact that with the isochrone fitting method one simply fits a curve to the points, whereas with the synthetic CMDs one has to reproduce the points

themselves, including morphology and quantity. The difference in modulus is, presumably, simply the consequence of the age difference.

Assuming a single slope Salpeter IMF, the mass of gas that formed the stars of the surveyed area of NGC 2099 between 0.6 and $100 M_\odot$ is $\simeq 2.6 \times 10^3 M_\odot$ with the BBC94 models, $2.5 \times 10^3 M_\odot$ and $3.1 \times 10^3 M_\odot$ with the FST and the FRANEC models, respectively.

5.3 NGC 2168

The cluster field contains 9298 *bona fide* stars. Our previous work on NGC 2168 (JSKIV) suffered due to the large size of the cluster ($R > 20'$). A very small blank field was constructed from the outer edges of the CFH12K CCD mosaic. In fact, some cluster members surely resided within the blank field, and therefore the cluster luminosity function could have been underestimated. Using synthetic CMDs, we find that we can only reproduce the observed stellar distribution in the CMD and the luminosity function if we use 500-600 stars down to $V = 19$. Using the blank field from the outer edges of the CCD subtracts off too many stars and forces a poor agreement between the theory and the observations. This confirms our initial suspicion that the cluster is larger than our aerial coverage. The synthetic CMDs shown here contain 550 stars brighter than $V = 19$.

For the synthetic CMD comparisons, we again use both Solar and subsolar metallicity models from each of FST, BBC94, and FRANEC. We immediately find that the subsolar metallicity models provide a much nicer agreement to the observations than Solar metallicity models. The Solar metallicity models not only predict an insufficient number of main-sequence stars just below the turn-off, they also contain very vertical upper main sequences. Besides, for ages as old as ~ 180 Myrs the turn-offs are slightly too faint, while for younger ages, < 120 Myrs, the turn-off has the proper luminosity but is severely underpopulated when compared to the observations. Flattening the IMF did not help the overall fit.

Figure 6 shows the best synthetic CMDs for NGC 2168. For the FST tracks (left), the models with maximum overshooting ($\zeta = 0.03$) and low metallicity ($Z = 0.006$) reproduce the data very nicely. These require a best fit distance modulus slightly smaller ($(m-M)_\odot = 9.6$) and a reddening slightly larger ($E(B-V) = 0.22$) than found in JSKIV. The differences can be most likely attributed to the lower metallicity (JSKIV uses $Z = 0.012$) that we chose in these com-

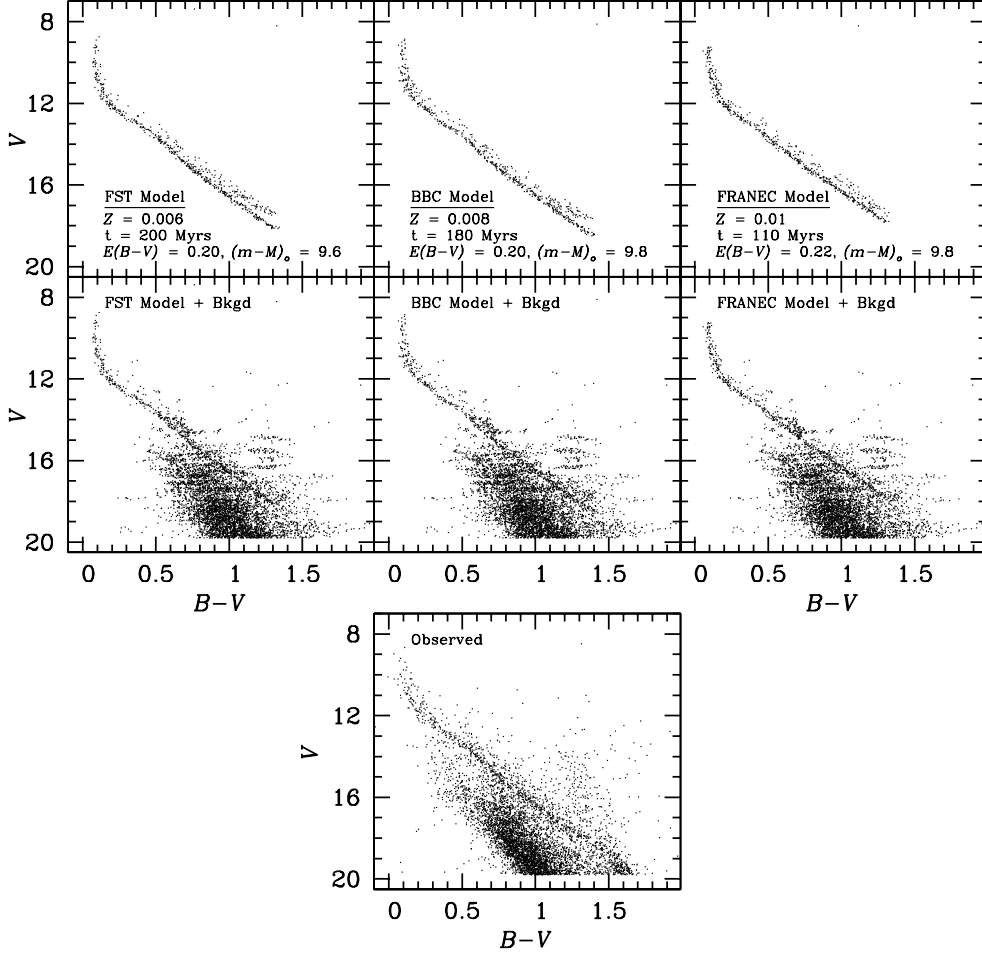


Figure 6. Synthetic CMDs with subsolar metallicities and a 30% binary fraction (random mass ratio), are shown for NGC 2168. The BBC94 tracks are found to provide the best agreement with the observations (bottom panel). The data has been truncated at the faintest magnitudes (see Figure 1 for full CMD). See §5.3 for more information.

parisons. The best age for this model is 200 Myrs, slightly older than what JSKIV found (180 Myrs). The absence of a population of post main-sequence stars coupled with the insensitivity of the turn-off luminosity and morphology with age in these models allows for a nice agreement between the theory and data with ages down to 120 Myrs.

The agreement is found to be not as good if we use the same metallicity FST models with slightly lower overshooting, $\zeta = 0.02$. At an age of 180 Myrs the turn-off is too faint, however, with younger ages (150 Myrs) we overpopulate the post main-sequence stars (five are seen). At 120 Myrs, the turn-off is too bright, hence this age is too young.

The BBC94 models for NGC 2168 are shown in the middle panel of Figure 6. The $Z = 0.08$ tracks are found to excellently reproduce both the CMD morphology and the number of stars in the different phases. The main-sequence curves are best fitted using $E(B-V) = 0.20$ and $(m-M)_0 = 9.8$. The best age estimate is found to be 180 Myrs. An age of 150 Myrs doesn't provide any post main-sequence stars whereas an age of 200 Myrs is too old as it predicts too many clump stars. The FRANEC models (right) predict too many post main-sequence stars for both adopted metallicities, $Z =$

0.01 and $Z = 0.02$. As summarised in JSKIV, many studies of NGC 2168 exist in the literature with none finding more than a few clump stars. The FRANEC models would require a very young age (110 Myrs) to fit the post main-sequence phases and this would in turn force a poor agreement in the turn-off region. The best fit model is, arguably, the one with age = 110 Myrs, $E(B-V) = 0.22$, and $(m-M)_0 = 9.8$.

Our best estimate for the NGC 2168 binary fraction is found to be $\sim 30\%$. This fraction puts a consistent number of stars, and sparse regions, on the red side of the cluster main-sequence in the synthetic CMDs. All CMDs shown in Figure 6 contain this binary fraction.

Comparing the resulting best synthetic CMDs with the observed one, it is clear that the predicted main sequence is too tight and slightly underpopulated at faint magnitudes ($V > 15$). As addressed earlier in §5.1, the tightness is a question of photometric errors, possible differential reddening, or metallicity spreads within the cluster. The underpopulation in this case is most likely related to the uncertain method we have used to infer the number of cluster members. Many tests that we have done indicate that we cannot attribute more stars to the cluster without getting too

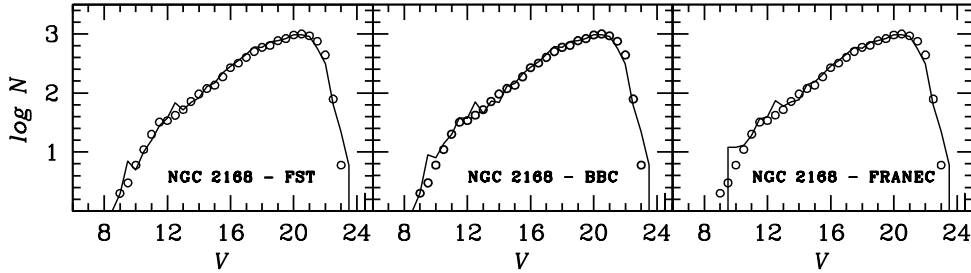


Figure 7. The empirical NGC 2168 luminosity function (open circles) is compared with the predicted luminosity function from the numerical simulations (solid line). See §5.3 for a discussion of these results.

many bright stars, both on the main sequence and in subsequent evolutionary phases. We also note here that $V = 19$ is the limiting magnitude of the numerical simulations for this cluster. This is related to the availability of photometric conversion tables (Bessell et al. 1998) for the adopted metallicities. With that said, it is remarkable how well the overall shape of the upper main sequence is reproduced. The ‘kinks’ and slope changes all fall in the correct place as dictated by the observations. This allows us to accurately determine the best fit parameters for NGC 2168. Interestingly, the best fit synthetic CMD for this cluster, the BBC94 model, provides an identical reddening, distance, and age to what we found using the FST isochrone in JSKIV. The FST synthetic CMD derived parameters are also in excellent agreement with our observations considering that the metallicities are slightly different.

Figure 7 shows the empirical luminosity function of the 9298 cluster field stars (empty circles) compared to the luminosity functions resulting from the sum of the synthetic stars of Figure 6 with the 8748 stars resulting by randomly multiplying the 1150 objects of the supposed blank field for an area normalisation factor. Clearly, a major side effect of the lack of an appropriate external field is that the comparison of the luminosity functions becomes only a matter of self-consistency and cannot be used for any consideration on mass segregation/evaporation. As mentioned above, the luminosity functions agree with the data only with 500-600 cluster members. One may think to improve the situation by steepening significantly the IMF (thus allowing for more stars in the fainter main sequence, without adding bright ones), but we consider it highly dangerous to modify the IMF without a good field subtraction. We stress that observations of a deep BV field offset from the centre of NGC 2168 by at least one degree would be very useful.

Assuming a single slope Salpeter IMF, the mass of gas that formed the stars of the surveyed area of NGC 2168 between 0.6 and $100 M_{\odot}$ is $\simeq 8.5 \times 10^2 M_{\odot}$ with the BBC94 models, $7.8 \times 10^2 M_{\odot}$ and $9.6 \times 10^2 M_{\odot}$ with the FST and the FRANEC models, respectively.

5.4 NGC 2323

The cluster field contains 11115 *bona fide* stars. Taking into account that 1) the blank field contains 5142 stars but covers an area 1.8 times smaller than the cluster field, 2) the mass of the available stellar models don’t allow synthetic stars fainter than $V \sim 18$, the synthetic CMDs have been initially

computed with 565 objects brighter than $V = 18$. A posteriori, we have however found that in this way we predict luminosity functions clearly overestimating the bright portion (where the cluster dominates) and underestimating the faint portion (where field contamination dominates). We empirically find that good luminosity functions are obtained only if the cluster contains 285 members brighter than $V = 18$, suggesting that the previously used blank field underestimated the actual contamination. Again observations of an external field of appropriate size would be crucial for a safer derivation of some of the cluster properties.

For the youngest cluster in this work, NGC 2323, the metallicity is known to be Solar and in fact, we find that the Solar metallicity tracks provide the best agreement to the data in this work. The most difficult parameter to fit in NGC 2323 is the cluster age. Although ages can be constrained from the turn-off morphology, the luminosity of the red giant clump is an alternative tool. NGC 2323 only shows two bright, red objects which are potential post main-sequence candidates. However, since these two objects do not have any membership probability from the literature, we can not trust them as cluster members. Furthermore, the turn-off itself is not heavily populated preventing an accurate determination of its luminosity. As we’ll see below, we find that models with a range of young ages are equally consistent with the observed distribution.

Figure 8 presents our best synthetic CMDs for NGC 2323. All of the shown cases are for Solar metallicity and assume a 30% binary fraction with random mass ratio.

The FST models (left) are found to perfectly reproduce the majority of the observed features. The agreement is also found to be independent of the adopted overshooting ($\zeta = 0.02$ or $\zeta = 0.03$). Although the age is slightly higher (by ~ 20 Myrs) in the higher overshooting case, the reddening, distance modulus and goodness of fit are the same. Our best parameters are therefore age = 130 Myrs, $E(B-V) = 0.22$, and $(m-M)_{\odot} = 10.0$ for $\zeta = 0.03$. However, ages between 120 and 180 Myrs are equally likely. We have chosen 130 Myrs as this age predicts a post main-sequence star where a real star (member or not) is indeed located on the CMD. Therefore, the results from this work for the FST models are identical to the parameters found in JSKIV. The BBC94 stellar tracks also perfectly reproduce features on the CMD of this cluster. For $E(B-V) = 0.22$, the best fit distance modulus is found to be $(m-M)_{\odot} = 10.2$. In practice, all ages between 80 and 150 Myrs fit the data equally well. We’ve again chosen 120 Myrs as the best age as it predicts a post main-sequence star

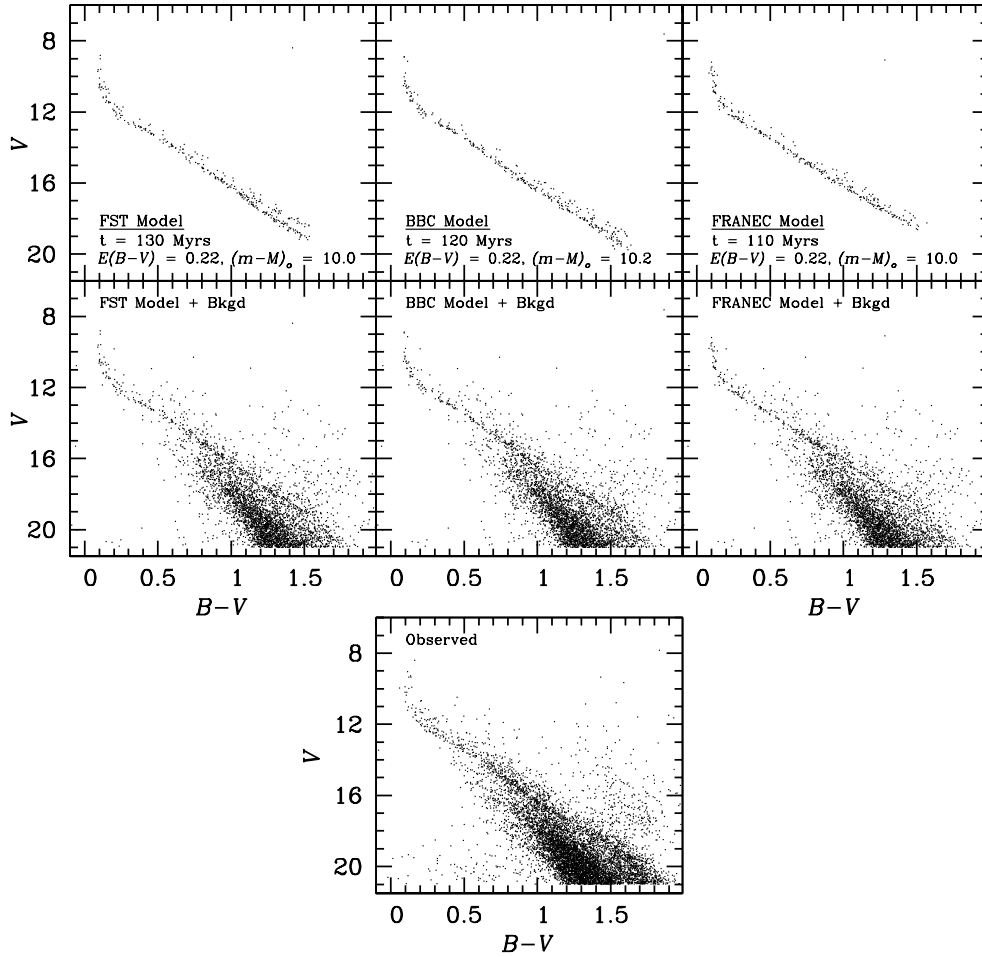


Figure 8. Synthetic CMDs with $Z = 0.02$ and a 30% binary fraction (random mass ratio), are shown for NGC 2323. The BBC94 tracks are found to provide the best agreement with the observations (bottom panel). The data has been truncated at the faintest magnitudes (see Figure 1 for full CMD). See §5.4 for more information.

in the correct location as dictated by the potential red giant in the data. The FRANEC models (right) predict a larger number of post main-sequence stars than the FST and BBC models. This is therefore inconsistent with the observational data. For Solar metallicity, the best compromise between the number of post main-sequence stars, the turn-off luminosity, and the shape of the upper main sequence is found for an age of 110 Myrs. The turn-off is still too faint, however, younger ages produce very vertical and blue upper main sequences. The best fit reddening is $E(B-V) = 0.22$ and the distance is $(m-M)_o = 10.0$. Since the results from these latter comparisons were not very satisfactory, we also tried a lower metallicity, $Z = 0.01$. The results are very similar, with an overproduction of post main-sequence stars and a worse shape to the upper main sequence.

Figure 9 shows the empirical luminosity function of the 11115 cluster field stars (empty circles) compared to the luminosity functions resulting from the sum of the synthetic stars of Figure 8 with the 10576 stars of the extrapolated blank field. As already discussed for NGC 2168, the lack of an appropriate estimate of the back/foreground stars doesn't allow for a critical analysis of the luminosity func-

tion. We can see, however, from Figure 8, that within the uncertainties, the selected models reproduce quite well the observed luminosity function.

Assuming a single slope Salpeter IMF, the mass of gas that formed the stars of the surveyed area of NGC 2323 between 0.6 and $100 M_\odot$ is $\simeq 4.8 \times 10^2 M_\odot$ with the BBC94 models, $4.3 \times 10^2 M_\odot$ and $5.0 \times 10^2 M_\odot$ with the FST and the FRANEC models, respectively.

6 DISCUSSION

Table 2 summarises the results described in the previous section and includes other information about the four clusters studied here. We recall that stellar models that include overshooting from convective regions imply older ages than models without overshooting. This explains why our ages resulting from the FST tracks with $\zeta=0.03$ are systematically older than those obtained with the BBC94 models and much older than those obtained with the FRANEC ones. It is interesting to notice that while the FST models with higher overshooting reproduce the data better than those

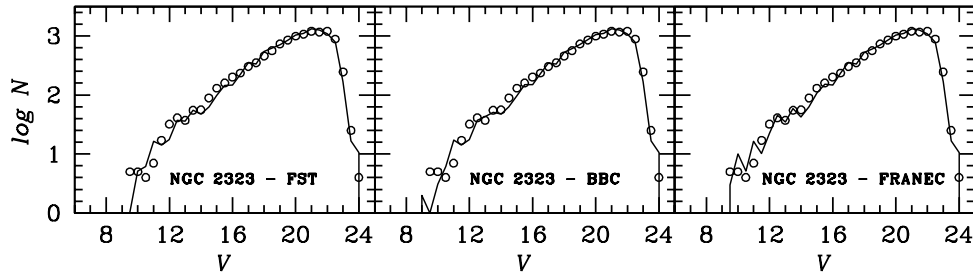


Figure 9. The empirical NGC 2323 luminosity function (open circles) is compared with the predicted luminosity function from the numerical simulations (solid line). See §5.4 for a discussion of these results.

with $\zeta=0.02$, the BBC94 models appear to be those in better overall agreement, in spite of having a formal overshooting somewhat lower than the FST $\zeta=0.03$ models. This indicates that what counts in the predictions of stellar evolution models is the combination of the many parameters and input physics. We find that in general the BBC94 models better reproduce both the morphological features and the numbers of stars in the various evolutionary phases of the observed clusters.

The excellent delineation of the various main-sequence curves and kinks allows us to put fairly stringent limits on both the reddening and the distance modulus of each cluster, independent of the age. Table 2 shows in fact that the variation of the values of these two quantities resulting from different sets of stellar tracks is quite small. This clearly helps to better define the age as well.

As discussed for the case of NGC 6819, the synthetic main sequences of all the four clusters are tighter than the observed main sequences when the formal photometric errors of the survey catalogues are assumed. To reproduce the observed width, the synthetic CMDs require either photometric errors of at least 0.01 magnitude even in the brighter bins or some other factors such as an internal metallicity spread or differential reddening.

The synthetic CMD tests clearly indicate that NGC 2168 is larger than previously thought and that our outer CCD blank field is not adequate. A similar problem, although to a lesser degree, may also exist in the NGC 2323 data set. Future deep photometry of these clusters should include separate blank field observations. Indeed, in spite of the great depth and excellent accuracy of our photometry, which allows us to measure the faintest, least massive stars of each cluster, the lack of appropriate decontamination fields has prevented us from safely deriving their present mass functions and, consequently, their IMF, mass segregation, and evaporation status.

The synthetic CMDs have allowed us to infer the astrated mass of each cluster. We find that although this does depend on the adopted set of stellar evolutionary tracks, it only varies within a factor 1.2 from the minimum to the maximum value obtained with the stellar models considered here. We have chosen to simply apply Salpeter’s single slope IMF for this exercise. We note, however, that increasing evidence suggests that the slope is most likely different (steeper for more massive stars, flatter for less massive ones, e.g., Kroupa 2002) beyond the range of masses, $2 - 10M_{\odot}$, originally analysed by Salpeter (1955). Although this simplistic

assumption introduces a systematic error in our estimates, it is not a large concern as we are not providing absolute values of star formation rates but rather just comparing relative rates for the four clusters.

Given the angular size of the observed field of view for each cluster (see Table 2), the actual area surveyed obviously depends on the adopted distance to the cluster. We have assumed both the intrinsic distance modulus and the astrated mass resulting from the best synthetic CMD comparisons, the BBC94 models. This corresponds to a distance from the Sun of 2754 pc for NGC 6819, 1259 pc for NGC 2099, 912 pc for NGC 2168, and 1096 pc for NGC 2323. The surveyed areas are then 182, 81, 56 and 72 pc^2 , respectively. The corresponding astrated mass per unit area is then 23.1, 32.1, 15.2 and 6.7 $M_{\odot}pc^{-2}$, equivalent to star formation rates of 4.6×10^{-6} , 6.4×10^{-6} , 3.0×10^{-6} , and $1.3 \times 10^{-6} M_{\odot}yr^{-1}pc^{-2}$, respectively. These values refer only to stars with masses included in the adopted sets of evolutionary tracks, namely from 0.6 to $100 M_{\odot}$. To derive total astrated masses and star formation rates, one should extrapolate down to $0.1 M_{\odot}$, following the preferred IMF. In practice, extrapolating Salpeter’s IMF down to $0.1 M_{\odot}$, we must multiply by a factor 2.05 the astrated masses and the rates. If, at the other extreme, we prefer to assume the positive slope +0.44 below $0.6 M_{\odot}$ suggested by Gould, Bahcall & Flynn (1997), then the above values must be multiplied only by 1.27.

There is a significant difference (more than a factor of four) in the star formation rates of our four clusters, the most active having been NGC 2099 and the least active NGC 2323, with no apparent relation with Galactic location. These rates are 2–3 orders of magnitude higher than the average star formation rate of field stars in the Solar neighbourhood, $(2 - 10) \times 10^{-9} M_{\odot}yr^{-1}pc^{-2}$ (e.g. Timmes, Woosley & Weaver 1995), and are comparable to those of the most active dwarf irregular and blue compact galaxies (e.g. Tosi 2003 and references therein). The survival factor of the stars formed in any cluster clearly depends both on age and on evaporation and NGC 6819 turns out to be the only one of the four clusters having suffered a reduction from the number of formed stars to that of the stars still alive and present in the studied area.

7 CONCLUSIONS

We re-derive key parameters for the four very rich open star clusters, NGC 6819, NGC 2099, NGC 2168, and NGC 2323. The parameters are measured by comparing high quality,

Table 2. Summary of Parameters and Results

| Parameter | Explanation | NGC 6819 | NGC 2099 | NGC 2168 | NGC 2323 |
|------------------------------------|------------------------------------|---|---|---|---|
| Position: | | | | | |
| α_{J2000} | RA | 19 ^h 41 ^m 17.7 ^s | 06 ^h 08 ^m 54.0 ^s | 06 ^h 08 ^m 54.0 ^s | 07 ^h 02 ^m 48.0 ^s |
| δ_{J2000} | declination | +40°11'17" | +24°20.0' | +24°20.0' | −08°22'36" |
| l_{J2000} | Galactic longitude | 73.98° | 177.65° | 186.58° | 221.67° |
| b_{J2000} | Galactic latitude | 8.47° | 3.09° | 2.18° | −1.24° |
| Distances: | | | | | |
| $(m-M)_V$ - Previous Study | apparent distance modulus | 12.30 ± 0.12 | 11.55 ± 0.13 | 10.42 ± 0.13 | 10.68 ± 0.14 |
| $(m-M)_V$ - FST ($\zeta = 0.03$) | apparent distance modulus | 12.31 | 11.52 | 10.22 | 10.68 |
| $(m-M)_V$ - BBC94 | apparent distance modulus | 12.57 | 11.62 | 10.42 | 10.88 |
| $(m-M)_V$ - FRANEC | apparent distance modulus | 12.47 | 11.42 | 10.48 | 10.68 |
| $E(B-V)$ - Previous Study | reddening | 0.10 | 0.21 | 0.20 | 0.22 |
| $E(B-V)$ - FST ($\zeta = 0.03$) | reddening | 0.10 | 0.36 | 0.20 | 0.22 |
| $E(B-V)$ - BBC94 | reddening | 0.12 | 0.36 | 0.20 | 0.22 |
| $E(B-V)$ - FRANEC | reddening | 0.15 | 0.36 | 0.22 | 0.22 |
| $(m-M)_o$ - Previous Study | true distance modulus | 11.99 ± 0.18 | 10.90 ± 0.16 | 9.80 ± 0.16 | 10.00 ± 0.17 |
| $(m-M)_o$ - FST ($\zeta = 0.03$) | true distance modulus | 12.0 | 10.40 | 9.60 | 10.00 |
| $(m-M)_o$ - BBC94 | true distance modulus | 12.2 | 10.50 | 9.80 | 10.20 |
| $(m-M)_o$ - FRANEC | true distance modulus | 12.0 | 10.30 | 9.80 | 10.00 |
| d - Previous Study | distance from Sun | 2500 ± $\frac{216}{199}$ pc | 1513 ± $\frac{146}{133}$ pc | 912 ± $\frac{70}{65}$ pc | 1000 ± $\frac{81}{75}$ pc |
| d - FST ($\zeta = 0.03$) | distance from Sun | 2512 pc | 1202 pc | 832 | 1000 |
| d - BBC94 | distance from Sun | 2754 pc | 1259 pc | 912 | 1096 |
| d - FRANEC | distance from Sun | 2512 pc | 1148 pc | 912 | 1000 |
| Age: | | | | | |
| t - Previous Study | isochrone fit age | 2.5 Gyrs | 520 Myrs | 180 Myrs | 130 Myrs |
| t - FST ($\zeta = 0.03$) | synthetic CMD age | 2.3 Gyrs | 520 Myrs | 200 Myrs | 130 Myrs |
| t - BBC94 | synthetic CMD age | 2.0 Gyrs | 430 Myrs | 180 Myrs | 120 Myrs |
| t - FRANEC | synthetic CMD age | 1.6-1.8 Gyrs | 400 Myrs | 110 Myrs | 110 Myrs |
| Metallicity: | | | | | |
| Z | heavy metal abundance ¹ | 0.02 | <0.02 | 0.012 | 0.020 |
| Binary Fraction | | | | | |
| Binaries | binary percentage | 20% | 20% | 30% | 30% |
| Size: | | | | | |
| Θ | angular diameter | 19' | 27'8 | >32' | 30' |
| D | linear diameter ² | 15.2 pc | 10.2 pc | >8.5 pc | 9.6 pc |
| M | mass of cluster ³ | 4000 M_\odot | 2500 M_\odot | 850 M_\odot | 480 M_\odot |

1. These values were not spectroscopically determined and reflect those used in the original isochrone fits.

2. Computed using the distances from the BBC94 results.

3. M is the mass of gas that formed stars between 0.6 and 100 M_\odot and is therefore only a lower limit to the total astrated mass.

deep empirical colour-magnitude diagrams with MonteCarlo simulations. The combination of comparing the morphology and number of stars in various evolutionary phases and cluster luminosity functions allows us to provide tight constraints on the reddening, distance, age and binary fraction for each cluster. In cases where the cluster metallicity is not certain, simulations with different abundances are also compared. In all cases the data are better reproduced when a fraction of unresolved binary systems between 20 and 30% is assumed. A summary of the results is given in Table 2.

The synthetic CMDs and LFs are generally found to be in excellent agreement with the observational data. This circumstance, combined with the fact that different sets of stel-

lar evolution tracks provide different values for the cluster parameters, confirms how important it is to use more than one set of models to estimate the theoretical uncertainties. It also shows that a homogeneous approach is crucial to derive reliable overall cluster properties, such as age-metallicity relations. In fact, cluster dating based on different stellar models may lead not only to different absolute ages, but also to different age ranking, with significant drawbacks on the interpretation of the cluster properties in terms of Galactic evolution.

Some discrepancies, such as the thickness of the main sequences *vis à vis* the size of the photometric errors, and the possibility that cluster stars may be contaminating our

blank field (particularly in the case of NGC 2168) are identified and discussed.

For each cluster, we also measure the astration mass (i.e., the total mass that went in all of the stars formed in the cluster) according to a single slope Salpeter IMF. From this, we calculate the star formation rate between $0.1\text{--}100 M_{\odot}$ to be 9.4×10^{-6} , 1.3×10^{-5} , 6.2×10^{-6} , and $2.7 \times 10^{-6} M_{\odot} \text{yr}^{-1} \text{pc}^{-2}$ for NGC 6819, NGC 2099, NGC 2168, and NGC 2323 respectively. These rates would be a factor 1.6 lower if the IMF below $0.6 M_{\odot}$ has a slope of +0.44, as inferred by Gould et al. (1997) from HST data, rather than Salpeter. The true value may in fact lie somewhere in between these two IMFs, as recently discussed e.g., by Chabrier (2003). In principle our data are deep enough to allow for a direct derivation of the cluster IMF; however, the four clusters are heavily contaminated by fore/background stars and the lack of appropriate decontamination fields has prevented us from a safe analysis of the star counts at the fainter magnitudes. The need of appropriate photometry in nearby fields is emphasised, also for the purpose of adequate studies of the clusters mass segregation/evaporation.

ACKNOWLEDGMENTS

We thank Paolo Ventura and Franca D'Antona for having provided their stellar models prior to publication. The bulk of the synthetic CMD code was originally written by Laura Greggio. J. S. K. received financial support during this work through an NSERC PGS-B graduate student research grant. This work has been partially funded through the Italian MIUR-Cofin-2003029437.

REFERENCES

- Andruzzi, G., Bragaglia, A., Tosi, M., Marconi, G. 2004, MNRAS, in press, astro-ph/0311249
- Aparicio, A., Bertelli, G., Chiosi, C., Garcia-Pelayo, J. M. 1990, A&A, 240, 262
- Barrado y Navascués, D., Deliyannis, C. P., & Stauffer, J. R. 2001, ApJ, 549, 452
- Bellazzini, M., Ibata, R., Monaco, L., Martin, N., Irwin, N.J. 2003, MNRAS, in press, astro-ph/0311119
- Bertelli, G., Bressan, A., Chiosi, C., Fagotto, F., & Nasi, E. 1994, A&AS, 106, 275
- Bertin, E., & Arnouts, S. 1995, A&AS, 117, 393
- Bessell, M. S., Castelli, F., & Plez, B. 1998, A&A, 333, 231
- Bragaglia, A., 2003, in *Stars in Galaxies*, M.Bellazzini, A.Buzzoni, S.Cassisi eds, Mem.S.A.It. in press
- Bragaglia, A., Carretta, E., Gratton, R. G., Tosi, M., Bonanno, G., Bruno, P., Cali, A., Claudi, R., Cosentino, R., Desidera, S., Farisato, G., Rebeschini, M., & Scuderi, S. 2001, AJ, 121, 327
- Bragaglia, A., & Tosi, M. 2003, MNRAS, 343, 306
- Bressan, A., Fagotto, F., Bertelli, G., & Chiosi, C. 1993, A&AS, 100, 647
- de Bruijne, J.H.J., Hoogerwerf, R. & de Zeeuw, P.T. 2001, A&A, 367, 111
- Canuto, V. M., & Mazzitelli, I. 1992, ApJ, 389, 724
- Carraro, G., Ng, Y.K., & Portinari, L. 1998, MNRAS, 296, 1045
- Chabrier, G. 2003, ApJ, 586, L133
- Dominguez, I., Chieffi, A., Limongi, M., & Straniero, O. 1999, ApJ, 524, 226
- Fagotto, F., Bressan, A., Bertelli, G., & Chiosi, C. 1994, A&AS, 105, 29
- French, R. S. 2003, private communication
- Freytag, B., Ludwig, H. G., & Steffen, M. 1996, A&A, 313, 497
- Friel, E.D. 1995, ARA&A, 33, 38
- Gould, A., Bahcall, J., & Flynn, C. 1997, ApJ, 482, 913
- Hauschildt, P. H., Allard, F., & Baron, E. 1999, ApJ, 512, 377
- Janes, K.A., & Phelps, R.L. 1994, AJ, 108, 1773
- Kalirai, J. S., Fahlman, G. G., Richer, H. B., & Ventura, P. 2003, AJ, accepted. (astro-ph/0306241)
- Kalirai, J. S., Ventura, P., Richer, H. B., Fahlman, G. G., D'Antona, F., & Marconi, G. 2001c, AJ, 122, 3239
- Kalirai, J. S., Richer, H. B., Fahlman, G. G., Cuillandre, J., Ventura, P., D'Antona, F., Bertin, E., Marconi, G., & Durrell, P. 2001b, AJ, 122, 266
- Kalirai, J.S., Richer, H.B., Fahlman, G.G., Cuillandre, J., Ventura, P., D'Antona, F., Bertin, E., Marconi, G., & Durrell, P. 2001a, AJ, 122, 257
- Kroupa, P. 2002, Science, 295, 82
- Landolt, A. U. 1992, ApJ, 104, 340
- Mermilliod, J. C., Huestamendia, G., del Rio, G., & Mayor, M. 1996, A&A, 307, 80
- Nilakshi, N., & Sagar, R. 2001, A&A, 381, 65
- Reid, I. N. 1999, ARA&A, 37, 191
- Salpeter, E. E. 1955, ApJ, 121, 161
- Sarrazine, A. R., Steinhauer, A. J. B., Deliyannis, C. P., Sarajedini, A., Baily, C. D., Kozhurina-Platais, V., von Hippel, T., & Platais, I. 2000, A&AS, 32, 742
- Skillman, E.D., & Gallart, C. 2002, PASP, 274, 535
- Timmes, F.X., Woosley, S.E., Weaver, T.A. 1995, ApJS, 98, 617
- Tolstoy, E., & Saha, A. 1996, ApJ, 46 2, 672
- Tosi, M. 2000, in *The chemical evolution of the Milky Way: Stars versus clusters*, F. Matteucci, F. Giovannelli eds, (Kluwer, Dordrecht), 255, 505
- Tosi, M. 2003, in *Stars in galaxies*, A. Buzzoni, S. Cassisi and M. Bellazzini eds, Mem.S.A.It in press (astro-ph/0305416)
- Tosi, M., Greggio, L., Marconi, G., & Focardi, P. 1991, AJ, 102, 951
- Twarog, B.A., Ashman, K.M., & Anthony-Twarog, B. 1997, AJ, 114, 2556
- Ventura, P., Zeppieri, A., Mazzitelli, I. & D'Antona, F. 1998, A&A, 334, 953
- Xiong, D.R. 1985, A&A, 150, 133

This paper has been typeset from a \TeX / \LaTeX file prepared by the author.